Chemical Physics 117 (1987) 149–162
North-Holland, Amsterdam

THE $A^1\Sigma^+$–$X^1\Sigma^+$ BAND SYSTEM OF THE KH AND KD MOLECULES

A. PARDO, J.J. CAMACHO, J.M.L. POYATO and E. MARTÍN

Departamento de Química-Física y Química-Cuántica, Facultad de Ciencias, C-XIV, Universidad Autónoma de Madrid, Cantoblanco, 28049 Madrid, Spain

Received 20 November 1986; in final form 13 March 1987

The molecular constants of the $A^1\Sigma^+$ and $X^1\Sigma^+$ states of the KH and KD molecules have been determined using mass relations correspondent to a normal isotope shift. For that calculation we have used data of the laser-induced fluorescence spectrum by the Ar^+ 4881 Å exciting line photographed in our laboratory, as well as previous data presented by other authors. From the spectroscopic terms, quantum-mechanical PMO–RKR–van der Waals hybrid potentials have been generated. Numerical calculations for the $A^1\Sigma^+$ and $X^1\Sigma^+$ states of the KH and KD species are compared with quantum-mechanical values obtained by numerical solution of the radial Schrödinger equation. Vibrational wavefunctions appropriate to the potential curves yield values of E_v and B_v which are in close agreement with the experimental results. The probability distribution functions and Franck–Condon factors for the $A^1\Sigma^+ \leftrightarrow X^1\Sigma^+$ band system have also been determined. It is observed that the anomalous behaviour of the A state is clearly revealed with a changed anharmonicity for the lowest vibrational levels.

1. Introduction

The $A^1\Sigma^+ \leftrightarrow X^1\Sigma^+$ electronic transition of potassium hydride has been spectroscopically analysed by various authors [1–8]. The most useful information is obtained from emission since in absorption the K_2 molecular spectrum strongly interferes. Although the band heads are not well defined, it is convenient to perform a rotational analysis previous to the vibrational analysis. In our laboratory we have also studied the fluorescence spectrum induced by the 4881 Å laser line of ArII [9]. This produces only the excitation transition ($v'' = 0$, $J'' = 5 \rightarrow v' = 7$, $J' = 6$), although important populations of vibrational states adjacent to the excited state are excited by collisions.

In this work we have obtained the molecular constants of the $X^1\Sigma^+$ and $A^1\Sigma^+$ states of KH and KD, using the mass relations corresponding to a normal isotope shift. They have been used for the lines identified in the fluorescence spectrum obtained in our laboratory [9], as well as for previous data [1–8]. We observed the typical anomalous behaviour of the $A^1\Sigma^+$ state of alkali hydrides.

From the molecular constants obtained, the potential energy curves have been determined. These are PMO–RKR–van der Walls hybrid potentials, obtained using the procedure that we have already proposed in the study of lithium hydride [10]. With these potentials, the radial Schrödinger equation is solved, producing a rather satisfactory agreement between the experimental and calculated values.

To provide simple and handy expressions, the potential energy curves have been fitted using analytic Padé-type approximants [10–13]. We also determined the probability density functions and Franck–Condon factors for the $A^1\Sigma^+ \leftrightarrow X^1\Sigma^+$ electronic transition. It is observed that the anomalous behaviour of the $A^1\Sigma^+$ state is clearly manifested in the levels $v' = 1$, 2, 3 and 4 resulting in probability functions with a changed anharmonicity.

2. Molecular constants

One of the main goals of spectroscopic analysis is the determination of molecular constants for the electronic states considered.

For the determination of the rotationless potentials we only need vibrational term values $G(v)$ and rotational constants B_v. Therefore, we calculated them by least-squares fits to expressions

$$\nu(v', v'') = T_e + \sum_{k=1} Y'_{k0}(v' + 1/2)^k - \sum_{l=1} Y''_{l0}(v'' + 1/2)^l \quad (1)$$

and

$$B_v = \sum_{k=0} Y_{k1}(v + 1/2)^k \quad (2)$$

for the vibrational transitions and rotational constants, respectively.

When spectral data of various isotopic species are used, if there is a normal isotope shift, the Dunham coefficients of different isotope species can be related through the equation [14]

$$Y^i_{jk}/Y_{jk} = \rho^{j+2k}. \quad (3)$$

Superscript i refers to the heaviest isotopic species and ρ is the ratio between the oscillation frequencies which is equivalent to $\rho = (\mu/\mu^i)^{1/2}$ where μ is the nuclear reduced mass of any isotope. More accurately eq. (3) [15] can be written

$$\frac{Y^i_{jk}}{Y_{jk}} = \rho^{j+2k}\left(1 + \frac{\beta_{jk}B_e^2}{\alpha_{jk}\omega_e^2}\frac{\mu - \mu^i}{\mu^i}\right), \quad (4)$$

where the terms α_{jk} and β_{jk} do not depend on the reduced mass. This correction arises when considering second-order effects in the Bohr–Sommerfeld semiclassical quantization condition. Taking into account that these corrections are inversally proportional to the reduced mass, they will be small for heavy systems and important for light molecules. In general it is not necessary to consider the higher-order correction terms since, in most molecules, the ratio B_e^2/ω_e^2 is usually on the order of 10^{-6} or less. For example, consider the value of this ratio for some molecules in the same electronic states: values for $Li_2(X^1\Sigma_g^+)$, Na_2 $(B^1\Pi_u)$, $CO(X^1\Sigma^+)$ and $I_2(B^3\Pi_{0u})$ are 3.7×10^{-6}, 1.0×10^{-6}, 7.9×10^{-7} and 5.2×10^{-8}, respectively.

For light molecules as alkali hydrides (specially for the A excited state) the ratio B_e^2/ω_e^2 is much larger. For example, for the $A^1\Sigma^+$ state of the ^{7}LiH, ^{22}NaH, ^{29}KH and RbH molecules the corresponding values are 1.4×10^{-4}, 3.0×10^{-5}, 2.6×10^{-5} and 2.8×10^{-5}, respectively. For the $X^1\Sigma_g^+$ and $B^1\Sigma_u^+$ states of H_2, this ratio is 1.9×10^{-4} and 2.2×10^{-4}, respectively.

The relation (4) must be used when trying to explain anomalous isotope shifts. These anomalous isotope shifts have been observed in the lithium hydride [16] whereas in the other alkali hydrides normal isotope shifts are observed.

Using programmes developed in our laboratory, we have determined the Dunham-type coefficients through least-squares fit. These programmes are in APL language since this language presents great advantages when working with matrices. Likewise, to estimate the precision of the fits we have calculated various statistical parameters of interest as: the total standard deviation of all analysed data, the multiple determination coefficient, the standard deviation of Dunham coefficients and the correlation matrix.

In addition to data from Almy [1], Bartky [3] and Giroud [6] we used the analysis of the laser-induced fluorescence spectrum done in our laboratory [9]. Moreover, we have considered the most recent data (Hussein et al. [8]) with information on vibrational levels near the dissociation.

In expressions (1) and (2), reduced quantum numbers referred to KD have been used being

$$\nu(v', v'') = T_e + \sum_{k=1} Y'_{k0}[(v' + 1/2)/\rho]^k - \sum_{l=1} Y''_{l0}[(v'' + 1/2)/\rho]^l, \quad (5)$$

where $\rho = 1$ for KD species and $\rho = [\mu(\mathrm{KH})/\mu(\mathrm{KD})]^{1/2} = 0.7162443$. For determining Y_{k1} we used the next equation:

$$B_v\rho^2 = \sum_{k=0} Y_{k1}[(v + 1/2)/\rho]^k, \quad (6)$$

where ρ takes the values above mentioned.

Table 1
Rotational and vibrational Dunham coefficients (cm^{-1}) isotopically combined for the $X^1\Sigma^+$ and $A^1\Sigma^+$ states of ^{39}KH. The number of figures retained are required to provide an accurate representation for the highest levels

j, k	$Y''_{jk}(X^1\Sigma^+)$	Standard error	$Y'_{jk}(A^1\Sigma^+)$	Standard error
T_e	1.906600750(+4)	3.49		
1, 0	9.874906992(+2)	0.49	2.201726585(+2)	1.8
2, 0	−1.613270476(+1)	0.25	7.640342154	0.34
3, 0	0.3326896132	4.9(−2)	−3.529548606(−1)	2.8(−2)
4, 0	−2.958809880(−2)	4.3(−3)	7.178000818(−3)	1.0(−4)
5, 0	1.633915560(−3)	1.8(−4)	−7.116511886(−5)	1.5(−6)
6, 0	−3.889951758(−5)	2.6(−6)		
0, 1	3.426084560	7.7(−3)	1.2097213842	3.4(−2)
1, 1	−9.515533645	7.6(−3)	6.848961540(−2)	1.4(−3)
2, 1	4.792381617(−3)	2.2(−4)	−7.166114364(−3)	1.7(−4)
3, 1	−7.084849043(−4)	2.5(−5)	2.725904672(−4)	8.9(−6)
4, 1	4.757402949(−5)	1.2(−6)	−4.017960245(−6)	1.5(−7)
5, 1	−1.183292046(−6)	2.2(−7)		

Using mass reduced quantum numbers, isotopically combined molecular constants were derived from least-squares fits to eqs. (5) and (6). Our best set of Dunham coefficients of the $X^1\Sigma^+$ and $A^1\Sigma^+$ states of KH species are summarized in table 1.

The molecular constants of both species correspond to a normal isotope shift described by eq. (3).

As in all alkali hydrides, we observed in the $A^1\Sigma^+$ state an anomalous behaviour in the vibrational and rotational structure for low vibrational levels. For potassium hydride there is no experimental evidence of an anomalous isotope shift which would necessitate adiabatic corrections in the molecular constants as was done with lithium hydride [16]. In this sense, it would be very interesting to perform a simultaneous analysis with the species ^{39}KH, ^{39}KD, ^{41}KH and ^{41}KD.

3. Potential energy curves

The potential energy curves have been constructed from the experimental results presented in table 1. The minimum zone of the potential energy curves has been represented, quite accurately, using the model of the perturbed Morse oscillator (PMO)

$$U_0(r) = D_e\left(y^2 + \sum_{i=4}^{12} b_i y^i\right), \tag{7}$$

where $y = 1 - \exp[-a(r - r_e)]$. The perturbative terms b_i have been determined using the expressions that connect them with Dunham coefficients according to the procedure described by Huffaker [17,18]. The PMO expansion presents superior convergence properties to the Dunham expansion although the energy terms of both models are expressed exactly in the same way. In the PMO model each Dunham coefficient is an infinite sum of terms

$$Y_{jk} = Y_{jk}^{(0)} + Y_{jk}^{(2)} + Y_{jk}^{(4)} + \ldots, \tag{8}$$

where the superscript refers to the relative power of σ^{-1}, where $\sigma = (2\mu D_e)^{1/2}/a\hbar$. The parameter σ corresponds approximately to the number of bound vibrational states of the Morse oscillator and therefore the terms of eq. (8) should decrease rapidly. The terms $Y_{jk}^{(0)}$ contain first-order WKB contributions, $Y_{jk}^{(2)}$ depend linearly on the second-order contributions in the WKB energy level condition etc.

The contributions of upper order are more important for light molecules since the smaller μ is the bigger is σ^{-1}. These modified Dunham coefficients ($Y_{jk}^{(2l)}$, $l = 0, 1, 2, \ldots$) have been calculated for the $A^1\Sigma^+$ and $X^1\Sigma^+$ states of KH. The results are presented in table 2. It is observed that these corrections are quite significant which is normal when working with light molecules. In this way we obtain for the vibrational and rotational molecular constants the values $\omega''_e = 988.114853\ cm^{-1}$ and

Table 2
Modified Dunham coefficients $Y_{jk}^{(2l)}$ for the $A^1\Sigma^+$ and $X^1\Sigma^+$ states of KH (in cm^{-1})

j	$Y_{j0}^{(0)}$	$Y_{j1}^{(0)}$	$Y_{j0}^{(2)}$	$Y_{j1}^{(2)}$	$Y_{j0}^{(4)}$	$Y_{j1}^{(4)}$
$X^1\Sigma^+$						
0	0.0	3.425227	0.56913	0.001026	0.12855	−0.000168
1	988.1148	−0.094933	−0.62816	−0.000430	0.00401	0.000208
2	−16.3599	0.004980	0.31962	−0.000188	−0.09241	
3	0.38094	−0.000821	−0.04825	0.000113		
4	−0.021226	0.0000475	−0.00836			
5	0.001634					
6	−0.0000389					
$A^1\Sigma^+$						
0	0.0	1.210880	2.08171	−0.001158	−0.03489	
1	220.6923	0.069302	−0.51961	−0.00812		
2	7.66641		−0.02607			

Table 3
PMO–RKR–van der Waals potential energy curve and eigenvalues for the $X^1\Sigma^+$ state of KH. $r_e'' = 2.238238$ Å. All b_i and eigenvalues are in cm^{-1}. C_i coefficients are in cm^{-1} Å^i

v	Experimental		r_+ (Å)	r_- (Å)	Eigenvalues	
	$G(v)+Y_{00}$	B_v			$G(v)+Y_{00}$	B_v
0	490.45	3.379619	2.443781	2.068404	490.36	3.379771
1	1446.62	3.291975	2.621484	1.962566	1446.61	3.292111
2	2372.79	3.208821	2.759037	1.897021	2372.87	3.208326
3	3269.90	3.127889	2.881307	1.847709	3270.13	3.126593
4	4138.59	3.047695	2.995720	1.807894	4139.16	3.045110
5	4979.31	2.967403	3.106223	1.775019	4979.86	2.963299
6	5792.35	2.886678	3.213930	1.746534	5792.61	2.881829
7	6578.00	2.805546	3.320393	1.721661	6578.24	2.801259
8	7336.47	2.724252	3.426530	1.699700	7336.76	2.719742
9	8067.96	2.643117	3.533019	1.680114	8068.08	2.639471
10	8772.61	2.562398	3.640440	1.662488	8772.53	2.559344
11	9450.43	2.482144	3.749325	1.646451	9449.95	2.479820
12	10101.26	2.402056	3.860320	1.631716	10100.40	2.399521
13	10724.58	2.321343	3.974404	1.618180	10723.39	2.318497
14	11319.47	2.238580	4.092670	1.605555	11318.04	2.234427
15	11884.36	2.151568	4.217071	1.593913	11882.91	2.145967
16	12416.86	2.057191	4.350044	1.583006	12415.51	2.050574
17	12913.57	1.951273	4.495851	1.573128	12912.40	1.944345
18	13369.75	1.828437	4.660538	1.564209	13368.80	1.822592
19	13779.14	1.681964	4.854503	1.556690	13778.25	1.679280
20	14133.56	1.503649	5.095446	1.550654	14132.60	1.505738
21	14422.64	1.283658	5.419041	1.546219	14421.65	1.290001
22	14633.40	1.010392	5.915213	1.542540	14632.69	1.008851
23	14749.93	0.670337	6.981041	1.530932	14754.09	0.689971

$a = 2.332582567$ Å
$D_e = 13097.6\ cm^{-1}$
$b_4 = 0.0814367400$
$b_5 = 0.3190011905$
$b_6 = -0.0803225988$
$b_7 = -0.3351466861$
$b_8 = 0.5254527368$
$b_9 = -0.0638957709$
$b_{10} = -0.5942048564$
$b_{11} = 1.4564848273$
$b_{12} = -0.1320718444$
$C_0 = 14783.8672$
$C_c = -2.519845364(+7)$
$C_8 = 2.603365672(+9)$
$C_{10} = -9.71108962(+10)$
$C_{12} = 1.015163053(+12)$

$B_e'' = 3.425227\ cm^{-2}$, while $\omega_e' = 220.692267\ cm^{-1}$ and $B_e' = 1.210880\ cm^{-1}$. For KH, using higher-order Dunham corrections we obtain $Y_{00}' = 2.047\ cm^{-1}$ whereas $Y_{00}'' = 0.698\ cm^{-1}$.

To determine the potential zone corresponding to the experimental vibrational levels we have used the RKR method including higher-order effects in the Bohr–Sommerfeld semiclassical condition.

In the RKR method we performed numerical

Table 4
PMO–RKR–van der Waals potential energy curve and eigenvalues for the $A^1\Sigma^+$ state of KH. $r_e' = 3.764441$ Å. All b_v and eigenvalues are in cm^{-1}. C_i coefficients are in cm^{-1} Å^i

V	Experimental		r_+ (Å)	r_- (Å)	Eigenvalues	
	$G(v)+Y_{00}$	B_v			$G(v)+Y_{00}$	B_v
0	114.00	1.242208	4.142318	3.363544	114.06	1.241570
1	348.34	1.297232	4.392787	3.076145	348.62	1.295078
2	594.99	1.340259	4.558124	2.892433	595.40	1.338006
3	852.15	1.372735	4.692654	2.754942	852.35	1.371818
4	1118.19	1.396003	4.811922	2.645693	1118.32	1.394883
5	1391.60	1.411315	4.922746	2.555938	1391.86	1.410144
6	1671.03	1.419823	5.028691	2.480548	1671.28	1.419508
7	1955.23	1.422586	5.131813	2.416176	1955.53	1.421927
8	2243.08	1.420562	5.233370	2.360483	2243.46	1.420129
9	2533.57	1.414617	5.334167	2.311758	2533.94	1.414798
10	2825.78	1.405517	5.434733	2.268696	2826.11	1.405513
11	3118.90	1.393935	5.535424	2.230281	3119.22	1.394278
12	3412.17	1.380445	5.636494	2.195704	3412.40	1.381183
13	3704.94	1.365525	5.738127	2.164313	3705.06	1.366300
14	3996.59	1.349557	5.840478	2.135579	3996.64	1.350161
15	4286.60	1.332827	5.943695	2.109084	4286.58	1.333592
16	4574.46	1.315524	6.047904	2.084462	4574.34	1.315945
17	4859.72	1.297741	6.153277	2.061448	4859.60	1.297408
18	5141.95	1.279473	6.260006	2.039827	5141.88	1.278501
19	5420.76	1.260621	6.368333	2.019448	5420.79	1.258825
20	5695.74	1.240988	6.478561	2.000213	5695.96	1.238188
21	5966.54	1.220280	6.591061	1.982075	5966.99	1.216337
22	6232.75	1.198109	6.706295	1.965039	6233.52	1.193500
23	6493.98	1.173988	6.824827	1.949162	6495.05	1.169451
24	6749.83	1.147335	6.947349	1.934544	6751.12	1.143595
25	6999.84	1.117471	7.074705	1.921353	7001.22	1.115876
26	7243.53	1.083621	7.207922	1.909806	7244.72	1.086020
27					7480.70	1.052657
28					7707.57	1.012537
29					7922.44	0.960600
30					8121.28	0.895525
31					8300.83	0.820244
32					8457.34	0.726322
33					8585.46	0.611427
34					8681.76	0.498065

$a = -0.748517604$ Å
$D_e = 18437.1\ cm^{-1}$
$b_4 = 8.40554463$
$b_5 = 12.3364648$
$b_6 = 13.6815461$
$b_7 = 285.659856$
$b_8 = -175{,}411008$
$b_9 = 1408.72498$
$b_{10} = 7708.07965$
$b_{11} = -26361.3620$
$b_{12} = 136989.282$
$C_0 = 8727.8633$
$C_6 = -1.017432381(+8)$
$C_8 = 3.7187236751(+10)$
$C_{10} = -3.888560964(+12)$
$C_{12} = 8.663515862(+13)$

integration of the Klein equations using Gauss–Legendre quadrature technique to avoid the singularities of the integrals.

Finally, for large internuclear distances, we used expansions in inverse powers of r that resemble a van der Waals-type interaction:

$$U_0(r) = C_0 + \sum_{i=6}^{12} C_i/r^i, \tag{9}$$

where i is an even number. These coefficients are obtained by least-squares fit from the last few RKR turning points.

Through the above described method, the electronic potentials of the $A^1\Sigma^+$ and $X^1\Sigma^+$ states of ^{39}KH have been obtained. To obtain the vibrational and rotational energies we have used the Dunham coefficients presented in table 1. The results are shown in table 3 and 4. In each of these tables are indicated the coefficients of the expansions (7) and (9) used for the zone of the minimum and large distances, respectively.

To determine the equilibrium internuclear distance we used the typical relation $r_e = \beta/\sqrt{B_e}$ where fourth-order correction effects are considered in the term $Y_{01}^{(4)}$ for the calculation of B_e and $\beta = (\hbar/4\pi c\mu)^{1/2}$.

Furthermore, to check the self-consistency of the proposed potentials we used a computer programme developed in our laboratory [19], in which the radial wave equation is solved numerically

$$(H_0 + H_{rot})\psi_{vJ}(r) = E_{vJ}\psi_{vJ}(r). \tag{10}$$

The programme performs a Householder orthogonal similarity transformation to obtain a tridiagonal form. It solves the eigenproblem using a simplified version of the implicit QR algorithm. To improve performance, eigenvalues are solved on reduced submatrices using the spliting technique. Eigenvectors are calculated directly by orthonormal transformations on the identity matrix.

$$\begin{aligned} H_0 &= -\beta^2\, \mathrm{d}^2/\mathrm{d}r^2 + U_0(r); \\ H_{rot} &= \beta^2 J(J+1)/r^2. \end{aligned} \tag{11}$$

In tables 3 and 4 are also given the calculated eigenvalues E_v and $B_v = \beta^2\langle\psi_v\,|\,1/r^2\,|\,\psi_v\rangle$ for each vibrational level obtained through solution of eq. (10). For this we use the hybrid potential $U_0(r)$ defined in each table where the different zones are connected through a seventh-order Lagrangian interpolation. From the known value $D_e'' = 14776 \pm 4$ cm^{-1} [8], $T_e = 19066 + 26$ cm^{-1} (see table 1) and the wave number corresponding to the atomic transition $\tilde{\nu}_{AT} = 13017 + 30$ cm^{-1} [20] we estimated $D_e' = 8727 + 60$ cm^{-1}. Taking into account this value for D_e' and the last RKR maximum turning points we calculated the asymptotic zone of $A^1\Sigma^+$ potential. Once the whole potential is determined we solve eq. (10) obtaining the energy eigenvalues and rotational constants for vibrational levels up to $v' = 35$. In this way we obtained more extense knowledge about vibrational levels not experimentally observed.

By assuming that the KH and KD potential are the same and solving eq. (10), the eigenvalues for A and X states of KD were determined (see table 5 observed a rather good agreement between the calculated and experimental values.

To present the previous potentials completely, we fitted these to an analytic Padé-type approximant [11–13,21]

$$U_0(z) = a_0 z^2 \left(1 + \sum_{i=1}^{18} d_i z^i\right)\left(1 + \sum_{i=1}^{20} e_i z^i\right)^{-1}, \tag{12}$$

where $z = (r - r_e)/r$. The results obtained for the $A^1\Sigma^+$ and $X^1\Sigma^+$ states of KH are presented in table 6 and 7, respectively. The dissociation energy D_e presented in these tables corresponds to the limit of the expression (12) when $z \to 1$.

To provide a qualitative picture of relative position of the various potentials for $A^1\Sigma^+$ and $X^1\Sigma^+$ states of some alkali hydrides (LiH, NaH, KH and RbH), we plotted them together in fig. 1. We obtained these potentials using the above described method.

Also indicated in fig. 1 are the attractive ionic potentials for LiH, NaH, KH and RbH.

When we take as zero of energies the minimum of the potentials energy curve of the ground state, expressing the energy in eV and the internuclear distance in Å, these ionic potentials are given by

$$U_{ion}(r) = A - 14.401/r, \tag{13}$$

Table 5
Experimental and eigenvalues for the $X^1\Sigma^+$ and $A^1\Sigma^+$ states of KD. All quantities are in cm^{-1}

v	$X^1\Sigma^+$				$A^1\Sigma^+$			
	experimental		eigenvalues		experimental		eigenvalues	
	$G(v)+Y_{00}$	B_v	$G(v)+Y_{00}$	B_v	$G(v)+Y_{00}$	B_v	$G(v)+Y_{00}$	B_v
0	352.29	1.740419	351.98	1.740292	81.86	0.632721	80.99	0.632867
1	1043.38	1.707575	1043.21	1.707597	246.98	0.654270	246.44	0.653794
2	1718.82	1.676229	1718.76	1.676240	418.83	0.672503	418.66	0.671508
3	2379.04	1.645857	2378.95	1.645636	596.72	0.687693	596.60	0.687239
4	3024.36	1.616059	3024.38	1.615665	779.99	0.700109	779.73	0.699960
5	3655.03	1.586537	3655.25	1.585747	968.03	0.710008	967.85	0.709456
6	4271.23	1.557088	4271.57	1.555842	1160.28	0.717633	1160.15	0.717362
7	4873.11	1.527586	4873.33	1.525540	1356.20	0.723213	1356.03	0.723130
8	5460.77	1.497972	5460.74	1.495520	1555.28	0.726967	1555.19	0.726575
9	6034.33	1.468235	6034.33	1.465808	1757.07	0.729098	1757.01	0.729005
10	6593.87	1.438405	6594.07	1.435763	1961.12	0.729797	1961.06	0.729745
11	7139.47	1.408533	7139.65	1.406080	2167.03	0.729242	2167.01	0.728979
12	7671.21	1.378680	7671.43	1.376528	2374.42	0.727600	2374.44	0.727662
13	8189.14	1.348907	8189.23	1.346965	2582.95	0.725020	2582.94	0.725015
14	8693.32	1.319252	8693.27	1.317660	2792.28	0.721644	2792.29	0.721605
15	9183.74	1.289726	9183.44	1.288162	3002.12	0.717596	3002.14	0.717717
16	9660.36	1.260293	9659.91	1.258735	3212.18	0.712990	3212.14	0.713207
17	10123.08	1.230859	10122.42	1.229164	3422.22	0.707925	3422.17	0.708003
18	10571.69	1.201257	10570.96	1.199080	3631.98	0.702489	3631.91	0.702742
19	11005.88	1.171234	11005.13	1.168695	3841.24	0.696756	3841.13	0.697057
20	11425.15	1.140439	11424.47	1.137238	4049.81	0.690786	4049.65	0.691008
21	11828.87	1.108405	11828.37	1.104634	4257.47	0.684628	4257.30	0.684777
22	12216.14	1.074538	12215.83	1.070270	4464.06	0.678316	4463.86	0.678575
23	12585.81	1.038104	12585.76	1.033280	4669.40	0.571872	4669.17	0.671948
24	12936.43	0.998214	12936.70	0.993112	4873.34	0.665305	4873.11	0.665200
25	13266.15	0.953809	13266.68	0.948740	5075.70	0.658311	5075.50	0.658383
26	13572.75	0.903650	13573.44	0.899012	5276.36	0.651773	5276.20	0.651388
27	13853.50	0.846300	13854.29	0.842345	5475.16	0.644761	5475.06	0.644084
28	14105.14	0.780113	14105.90	0.777598	5671.97	0.637530	5671.97	0.636471
29	14323.83	0.703221	14324.46	0.702333	5866.64	0.630026	5866.78	0.628759
30	14505.04	0.613516	14505.63	0.613183	6059.04	0.622178	6059.31	0.620670
31	14643.50	0.508642	14643.87	0.503495	6249.01	0.613905	6249.46	0.612088
32	14733.13	0.385976	14733.94	0.371404	6436.43	0.605112	6437.05	0.603134
33					6621.12	0.595689	6621.92	0.593756
34					6802.94	0.585515	6803.89	0.583928
35					6981.72	0.574457	5982.74	0.573548
36					7157.27	0.562367	7158.27	0.562487
37							7330.22	0.550725
38							7498.16	0.537919
39							7661.42	0.523051
40							7818.80	0.504906
41							7968.81	0.483383
42							8110.23	0.459754
43							8242.11	0.432942
44							8362.72	0.401655
45							8470.55	0.366121
46							8563.54	0.323957
47							8639.48	0.274763
48							8698.67	0.238579

Table 6
Coefficients of the Padé approximant for the $A^1\Sigma^+$ state of the KH molecule. All values are given in cm^{-1}

i	d_i	e_i
1	−0.7425226393	−3.42613306
2	−30.04295526	−30.53377841
3	131.4745085	217.2359345
4	−20.87503557	−275.8834708
5	−853.8832021	−1159.807518
6	803.0052027	3101.152343
7	2463.075284	2135.245535
8	−2439.97486	−12284.05968
9	−3639.554	170.7412211
10	2067.294893	28590.05196
11	498.8125069	−6847.625931
12	2399.086219	−45433.75314
13	9422.06311	9536.180259
14	−3085.506236	50973.72413
15	−15598.00982	1327.057722
16	−3695.978606	−34953.0406
17	6677.639832	−13098.91938
18	3102.946491	7743.524732
19		6683.57239
20		1528.172284

$a_0 = 10090.78465$
$D_e = 8726.08$
standard deviation = 0.087568
regression coefficient = 0.9999981

Table 7
Coefficients of the Padé approximant for the $X^1\Sigma^+$ state of the KH molecule. All values are given in cm^{-1}

i	d_i	e_i
1	0.9519467256	1.275733179
2	−38.05390579	−37.20044.34
3	−23.06975888	−37.55311598
4	570.3483706	541.7379895
5	121.7180018	423.7528854
6	−46.03.924427	−4267.081023
7	1291.786465	−2739.183047
8	22900.54685	21686.19923
9	−22858.04185	13767.82339
10	−69571.11258	−80167.26959
11	165831.6615	−66464.66218
12	75534.02351	226271.9054
13	−532239.9984	317845.5201
14	272182.3807	−539003.0731
15	762556.8684	−1163666.962
16	−852473.3337	1397157.954
17	−61479.28089	2137399.835
18	263812.8828	−2747177.418
19		−804760.6286
20		1343957.499

$a_0 = 71276.36564$
$D_e = 14776.01787$
standard deviation = 0.05691
regression coefficient = 0.9999995986

where A depends on the molecule (MH),

$$A = D_e'' + \mathrm{IP(M)} - \mathrm{EA(H)} \qquad (14)$$

The ionization potential of M and the electron affinity of H [20] used in these calculations are given by

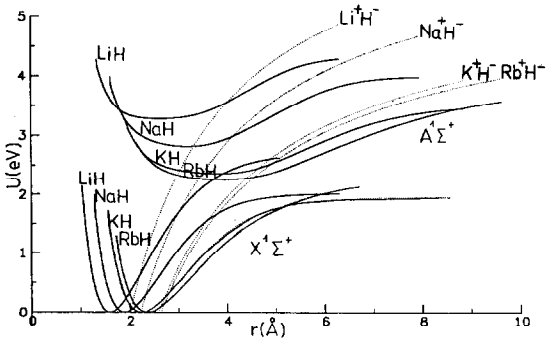

Fig. 1. PMO–RKR–van der Waals potential energy curves (in eV and Å) for the $A^1\Sigma^+$ and $X^1\Sigma^+$ states of LiH, NaH, KH and RbH. Also included are the attractive ionic curves for each hydride.

$$A(\mathrm{LiH}) = 2.515 + 5.392 - 0.747 = 7.16 \text{ eV},$$
$$A(\mathrm{NaH}) = 2.092 + 5.139 - 0.747 = 6.484 \text{ eV},$$
$$A(\mathrm{KH}) = 1.832 + 4.341 - 0.747 = 5.426 \text{ eV},$$
$$A(\mathrm{RbH}) = 2.033 + 4.177 - 0.747 = 5.463 \text{ eV}.$$

Taking into account that the smaller is the difference IP(M) − EA(H), the bigger the ionic contribution will be with respect to the covalent contribution, then LiH will have a bigger covalent contribution than the sodium, potassium and ribudium hydrides, these last presenting a similar behaviour.

At small internuclear distances we have to include in the expression (13) a Born (B/r^n) or Born–Mayer-type ($B'\exp(-r/a')$ repulsive term.

The $A^1\Sigma^+$ states of the alkali hydrides are of considerable interest because the $\Delta G(v + 1/2)$ and B_v values do not show the normally expected decrease with increasing v. Instead they rise initially before the normal decrease sets in, yielding

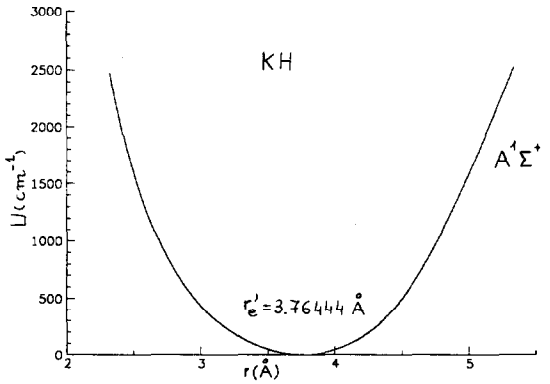

Fig. 2. Zone of the $A^2\Sigma^+$ potential of KH that shows a reversed anharmonicity.

anomalous negative values for $\omega_e x_e$ and α_e. Mulliken [22] has attributed these facts to the unusual shape of their potential energy curves. According to him the $A^1\Sigma^+$ and $X^1\Sigma^+$ states of an alkali hydride molecule arise from an interaction between the two $^1\Sigma^+$ states: one homopolar and derived from unexcited neutral atoms, the other ionic and derived from M^+ and H^-. Then the exceptional shape of the $A^1\Sigma^+$ potential curve would be due to an avoided crossing of the zero-order curves of MH and M^+H^-. In the case of KH the crossing between the calculated $A^1\Sigma^+$ potential and the ionic potential happens if $r_e =$ 4.635 Å which corresponds to an energy zone for v' between 1 and 2. This fact causes the potential of the $A^1\Sigma^+$ state to be very open (the minimum is not clearly differentiated) with a changed asymmetry in the zone of low vibrational levels.

To detail these facts more clearly we plot in fig. 2 the the zone of the $A^1\Sigma^+$ potential of KH that presents a changed anharmonicity. It can be observed that the potential, for equal shifts on both sides of the minimum, rises more rapidly in the right zone than in the left. This anomalous zone corresponds to a quite wide range of $2.32 < r <$ 5.34 Å.

4. Probability density distributions and Franck–Condon factors for the band system $A^1\Sigma^+ \leftrightarrow X^1\Sigma^+$

As mentioned previously, by solving the wave equation we obtain the eigenfunctions $\psi_{vJ}(r)$ for each state (v, J). The $J = 0$ eigenfunctions ψ_{v0} form an orthonormal set. To provide an idea of the most probable positions of the system in the different states, we present in figs. 3 and 4 the probability density functions $|\psi_v(r)|^2$ for some vibrational levels of KH. The values of the internuclear distance correspond to the zones of definition of the potentials, that is to say, for the $X^1\Sigma^+$ state from 1.45 to 8.59 Å and for the $A^1\Sigma^+$ state from 1.73 to 8.87 Å. These ranges were chosen to guarantee that the wavefunctions vanish for r going to zero and to infinity.

The anomalous behaviour of the $A^1\Sigma^+$ state may be observed in probability density functions for the levels $v' = 1$, 2, 3 and 4. For these levels it is more probable to find the system in positions near the minimum turning point than near the maximum turning point. This fact reveals the changed asymmetry of the potential in this zone with respect to the usual behaviour. For upper vibrational levels of the $A^1\Sigma^+$ state we obtain probability distribution functions corresponding to a potential with a normal anharmonicity. These same characteristics have been observed, although to a lesser extent, in NaH and RbH [23]. For the $A^1\Sigma^+$ state of LiH we do not observe this behaviour of the potential and of the probability density functions. To explain this possible discrepancy we have taken into account the normal anharmonic behaviour in a normal electronic state, physically stable, in which exists a normal anharmonicity manifested with a decrease of the vibrational spacing and a progressive increase of the effective rotational constants which leads to dissociation. If we take into account the $A^1\Sigma^+$ anomalous states of the alkali hydrides and we consider the crossings of the actual potentials with the ionic potential (see fig. 1), we can see that in the KH, NaH, and RbH that crossing arises between $v' = 1$–2, $v' = 3$–4 and $v' = 0$–1, respectively. On the contrary for LiH this crossing happens toward $v' = 6$–7.

As mentioned above, Mulliken's explanation [22] for the anomalous character of the $A^1\Sigma^+$ states and their anharmonicity constants is the avoided crossing between the ionic potential and the covalent potential. Taking into account where the crossing between the ionic and actual potential

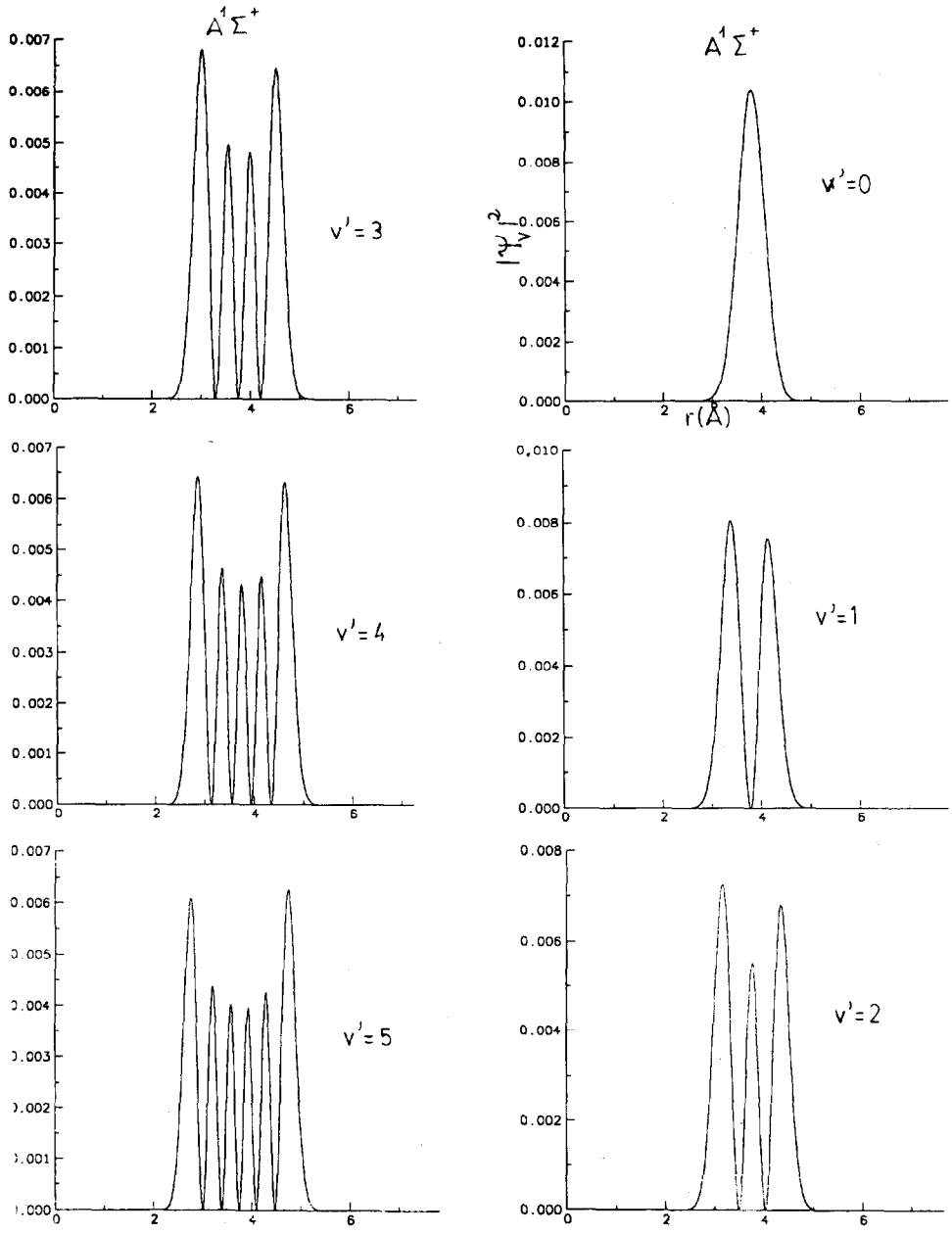

Fig. 3. Probability density distributions of the $A^1\Sigma^+$ state for the levels: $v' = 0$, 1, 2, 3, 4 and 5.

happens we can consider the following points:

(i) When the crossing is in low vibrational levels, and where the normal anharmonicity is small, the reversed anharmonicity of the avoided crossing prevails over the normal anharmonicity (KH, NaH and RbH cases).

(ii) When the crossing occurs in high vibrational levels, where the normal anharmonicity is big, the latter prevails and the probability functions and electronic potentials show a normal anharmonicity behaviour (LiH case).

For the $X^1\Sigma^+$ state we obtain sharper probabil-

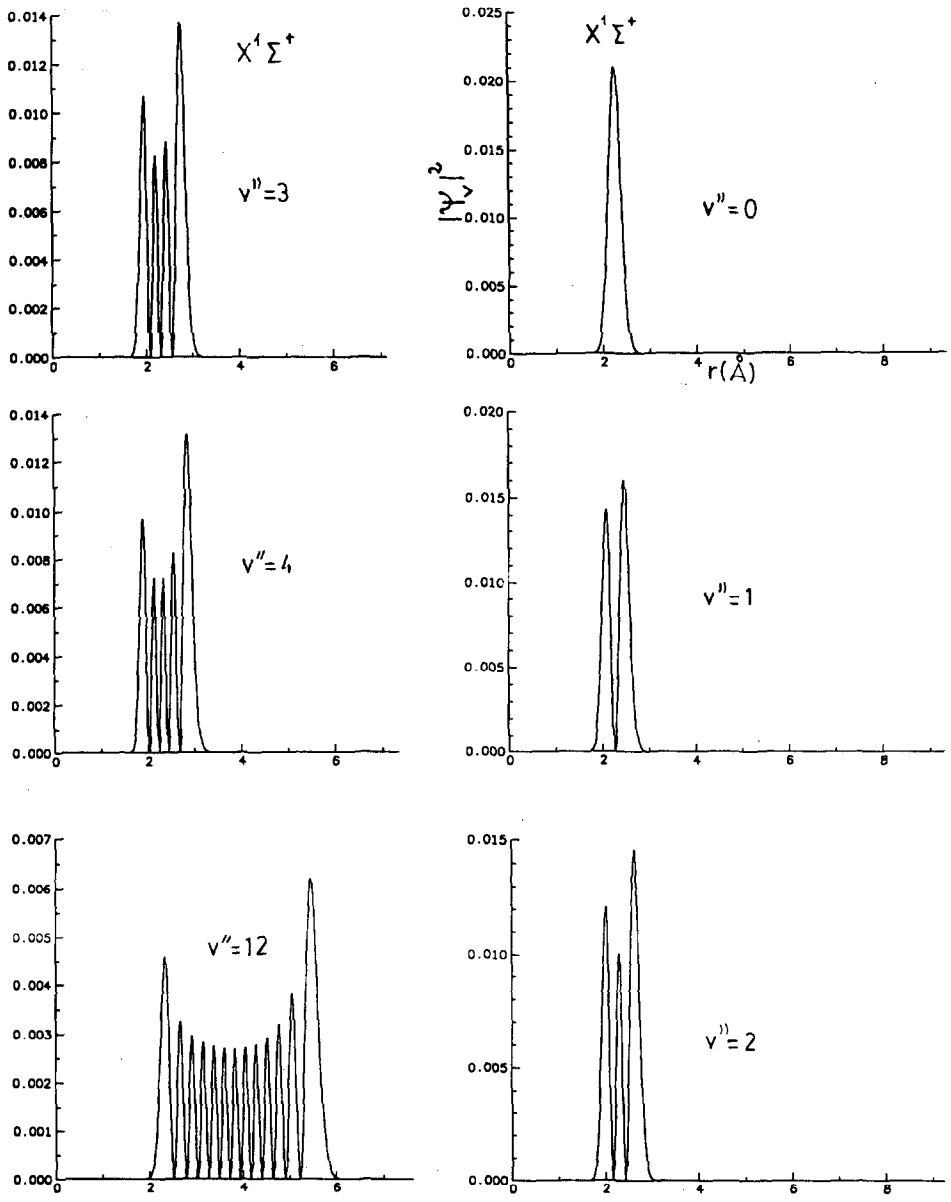

Fig. 4. Probability density distributions of the $X^1\Sigma^+$ state for the levels: $v'' = 0$, 1, 2, 3, 4 and 12.

ity density distributions than in the case of the $A^1\Sigma^+$ state representing a situation of stronger bounding and with a normal behaviour in the whole range of vibrational levels (fig. 4).

Franck–Condon factors for the $A^1\Sigma^+ \leftrightarrow X^1\Sigma^+$ band system have been determined using the wavefunctions (table 8). To provide an idea of the values obtained we show in fig. 5 the tridimensional graphic of Franck–Condon factors for the KH molecule. This intensity distribution is quite similar in all the alkali hydrides ($r_e' \gg r_e''$) with long fluorescence series. Besides it usually hap-

Table 8
Franck–Condon factors of the $A^1\Sigma^+ \leftrightarrow X^1\Sigma^+$ system of the KH molecule for $J' = J'' = 0$

v'	$v''=0$	$v''=1$	$v''=2$	$v''=3$	$v''=4$	$v''=5$	$v''=6$	$v''=7$	$v''=8$	$v''=9$	$v''=10$	$v''=11$
0	4E−6	0.000045	0.0027	0.0011	0.0036	0.0096	0.022	0.042	0.072	0.11	0.14	0.16
1	0.000065	0.00062	0.003	0.01	0.026	0.051	0.083	0.11	0.11	0.076	0.029	0.0006
2	0.0049	0.0038	0.015	0.038	0.071	0.097	0.093	0.055	0.011	0.035	0.042	0.079
3	0.0022	0.014	0.042	0.078	0.095	0.07	0.02	0.00071	0.034	0.068	0.046	0.0033
4	0.0072	0.035	0.076	0.093	0.058	0.0078	0.0092	0.052	0.056	0.011	0.0078	0.053
5	0.018	0.063	0.093	0.06	0.0062	0.014	0.056	0.041	0.0011	0.025	0.054	0.015
6	0.035	0.088	0.076	0.013	0.01	0.054	0.036	7.9E−6	0.033	0.045	0.003	0.024
7	0.057	0.095	0.036	0.0017	0.046	0.04	0.00018	0.032	0.04	0.0007	0.03	0.037
8	0.08	0.081	0.005	0.028	0.05	0.0037	0.024	0.041	0.0013	0.028	0.032	0.00035
9	0.099	0.051	0.0029	0.053	0.019	0.0095	0.044	0.0058	0.02	0.034	0.000021	0.035
10	0.11	0.02	0.025	0.046	0.000018	0.038	0.019	0.0082	0.038	0.0015	0.028	0.019
11	0.11	0.025	0.048	0.02	0.014	0.038	2.8E−5	0.035	0.011	0.016	0.028	0.0019
12	0.11	0.0017	0.055	0.0013	0.037	0.013	0.016	0.028	0.0024	0.033	0.00075	0.029
13	0.093	0.015	0.043	0.0048	0.04	0.000012	0.035	0.0037	0.025	0.012	0.014	0.02
14	0.077	0.034	0.023	0.023	0.022	0.012	0.026	0.0043	0.029	0.00054	0.029	0.000092
15	0.061	0.052	0.0061	0.038	0.0042	0.03	0.0062	0.023	0.0094	0.018	0.012	0.014
16	0.046	0.064	2.4E−7	0.041	0.0008	0.033	0.00065	0.029	0.00024	0.027	0.000079	0.026
17	0.033	0.068	0.0054	0.031	0.012	0.02	0.013	0.016	0.013	0.014	0.013	0.011
18	0.023	0.066	0.018	0.016	0.026	0.0049	0.026	0.0017	0.025	0.00044	0.024	3.8E−6
19	0.016	0.059	0.033	0.0037	0.033	0.00011	0.027	0.0023	0.021	0.0056	0.016	0.0099
20	0.01	0.049	0.045	0.000029	0.03	0.0069	0.017	0.014	0.0077	0.019	0.0022	0.021
21	0.0067	0.039	0.052	0.0045	0.02	0.018	0.0045	0.023	0.00007	0.022	0.0018	0.016
22	0.0042	0.03	0.053	0.014	0.0086	0.026	4.2E−6	0.022	0.0044	0.013	0.012	0.041
23	0.0026	0.022	0.05	0.025	0.0014	0.027	0.0043	0.013	0.014	0.0028	0.019	0.00023
24	0.0016	0.016	0.044	0.035	0.0003	0.021	0.013	0.004	0.02	0.00029	0.016	0.0069
25	0.00093	0.011	0.037	0.04	0.0045	0.012	0.02	0.000025	0.019	0.0059	0.015	0.007
26	0.00054	0.0072	0.03	0.042	0.012	0.0045	0.023	0.0024	0.011	0.014	0.00067	0.016
27	0.00031	0.0048	0.023	0.041	0.019	0.00048	0.02	0.0084	0.004	0.017	0.00099	0.01
28	0.00017	0.0031	0.017	0.037	0.026	0.00043	0.014	0.014	0.00025	0.015	0.0059	0.0036
29	0.000095	0.0019	0.012	0.031	0.029	0.0032	0.0077	0.017	0.00073	0.01	0.011	0.00017
30	0.000051	0.0012	0.0086	0.025	0.029	0.007	0.003	0.016	0.036	0.0047	0.013	0.00081
31	0.000028	0.00075	0.006	0.02	0.027	0.01	0.00063	0.013	0.0064	0.0013	0.012	0.0034
32	0.000015	0.00046	0.004	0.015	0.023	0.012	5.9E−7	0.009	0.0078	0.000081	0.0086	0.0054
33	8E−6	0.00027	0.0026	0.01	0.018	0.011	0.00024	0.0056	0.0074	0.000095	0.0054	0.0058
34	4.3E−6	0.00016	0.0016	0.0068	0.013	0.0092	0.00056	0.0032	0.0059	0.00038	0.0031	0.005

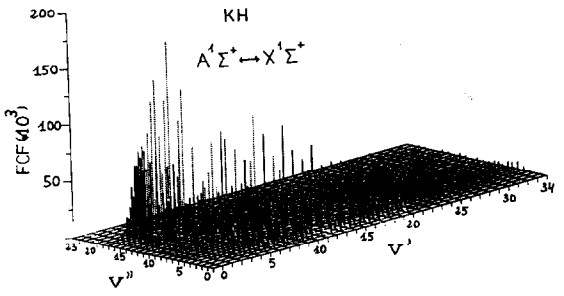

Fig. 5. Tridimensional graphics of the Franck–Condon factors for the $A^1\Sigma^+ - X^1\Sigma^+$ band system of KH.

pens that the low vibrational levels of $A^1\Sigma^+$ states are hardly detectable since they have high intensity factors only for big values of v''.

Acknowledgement

This work was carried out under the sponsorship of the Comisión Asesora de Investigación Científica y Técnica, Spain, Project 1203/83.

$v''=12$	$v''=13$	$v''=14$	$v''=15$	$v''=16$	$v''=17$	$v''=18$	$v''=19$	$v''=20$	$v''=21$	$v''=22$	$v''=23$
0.15	0.13	0.088	0.048	0.02	0.005	0.00052	1.5E−7	7.9E−7	1.2E−7	1.2E−7	9.2E−8
0.018	0.075	0.13	0.14	0.96	0.042	0.0085	0.00023	0.00009	1.8E−6	5.1E−6	1.8E−6
0.063	0.013	0.0077	0.077	0.14	0.13	0.052	0.0054	0.0002	0.00013	0.000051	8.4E−6
0.019	0.068	0.056	0.0027	0.041	0.15	0.15	0.043	0.00013	0.013	0.00013	1.4E−6
0.047	0.0021	0.029	0.07	0.017	0.03	0.17	0.15	0.014	0.0044	1E−6	0.0001
0.0082	0.054	0.028	0.0047	0.062	0.024	0.04	0.22	0.1	0.002	0.0032	0.0021
0.047	0.004	0.027	0.047	0.000058	0.052	0.017	0.091	0.26	0.012	0.022	0.0053
1.6E−6	0.038	0.026	0.0059	0.049	0.0023	0.044	0.0018	0.21	0.15	0.033	0.00074
0.038	0.016	0.012	0.04	0.000024	0.044	0.003	0.034	0.02	0.31	0.0004	0.017
0.015	0.013	0.035	0.00042	0.04	0.0015	0.039	0.0014	0.011	0.17	0.087	0.081
0.0083	0.034	0.000054	0.036	0.0024	0.033	0.0027	0.037	0.00047	0.011	0.21	0.056
0.034	0.00091	0.03	0.0061	0.026	0.008	0.027	0.0013	0.04	0.0053	0.11	0.000057
0.0073	0.021	0.014	0.015	0.017	0.015	0.011	0.023	0.0003	0.059	0.041	0.013
0.0069	0.025	0.0035	0.026	0.0035	0.023	0.0093	0.0095	0.019	0.019	0.011	0.0039
0.028	0.00078	0.027	0.00068	0.027	0.000065	0.023	0.0074	0.0057	0.0051	0.12	0.021
0.014	0.013	0.012	0.015	0.0076	0.02	0.00053	0.02	0.0087	0.0037	0.018	0.1
0.00013	0.025	0.00079	0.022	0.0042	0.014	0.014	0.0011	0.016	0.016	0.019	0.076
0.015	0.0076	0.018	0.0027	0.022	0.00015	0.017	0.01	0.00053	0.0066	0.055	0.054
0.023	0.0011	0.019	0.0057	0.011	0.015	0.00054	0.016	0.009	0.000023	0.0037	0.13
0.0094	0.015	0.003	0.02	0.00011	0.016	0.0087	0.0016	0.013	0.01	0.002	0.091
8.9E−8	0.02	0.0028	0.013	0.012	0.0017	0.017	0.005	0.0014	0.0078	0.022	0.049
0.0079	0.0076	0.015	0.00053	0.017	0.0041	0.0053	0.014	0.037	0.00045	0.000061	0.096
0.018	2E−8	0.0017	0.005	0.0064	0.015	0.00058	0.0072	0.012	0.004	0.00064	0.046
0.016	0.0064	0.0059	0.015	0.000061	0.012	0.0096	5.1E−6	0.0068	0.004	0.0082	0.025
0.0059	0.015	2.8E−6	0.014	0.007	0.0019	0.013	0.0054	0.00016	0.0047	0.0031	0.046
0.000068	0.015	0.052	0.0044	0.014	0.0012	0.0056	0.011	0.0032	0.000055	0.0029	0.0061
0.0031	0.0072	0.013	9.1E−6	0.011	0.0083	0.000064	0.0076	0.0086	0.0025	0.00023	0.0084
0.0099	0.00081	0.014	0.0041	0.0032	0.012	0.003	0.0013	0.073	0.0063	0.002	0.0044
0.014	0.0008	0.0081	0.01	8.1E−6	0.0081	0.0085	0.00051	0.0023	0.0056	0.0043	0.0013
0.012	0.0051	0.0021	0.012	0.0028	0.0023	0.0094	0.0044	1.1E−6	0.0021	0.0033	0.001
0.007	0.0088	1.6E−6	0.0082	0.0069	3.7E−6	0.0058	0.0071	0.0017	0.000064	0.00098	0.0025
0.0027	0.0096	0.0012	0.0038	0.0084	0.0012	0.002	0.0065	0.004	0.00056	0.000048	0.00021
0.0005	0.0077	0.0032	0.001	0.007	0.0032	0.00017	0.0041	0.0047	0.0018	0.00019	0.00011
1.9E−8	0.005	0.004	0.000059	0.0046	0.004	0.000087	0.0019	0.0037	0.0023	0.00068	0.00017
0.00016	0.0029	0.0037	0.000046	0.0026	0.0035	0.00044	0.00068	0.0024	0.0021	0.00088	0.00014

References

[1] G.M. Almy and D. Hause, Phys. Rev. 42 (1932) 242; G.M. Almy and A.C. Berler, Phys. Rev. 61 (1942) 476.

[2] T. Hori, Mem. Ryojun Coll. Eng. 6 (1933) 1.

[3] I.R. Bartky, J. Mol. Spectry. 21 (1966) 1.

[4] P. Cruse and R.N. Zare, J. Chem. Phys. 60 (1974) 1182.

[5] S.C. Yang, Y.K. Hsieh, K.K. Verma and W.C. Stwalley, J. Mol. Spectry. 83 (1980) 304.

[6] M. Giroud and O. Nedelec, J. Chem. Phys. 83 (1980) 304.

[7] N.N. Haese, D.J. Liu and R.S. Altman, J. Chem. Phys. 81 (1984) 3766.

[8] K. Hussein, C. Effantin, J. d'Incan, J. Verges and R.F. Barrow, Chem. Phys. Letters 124 (1986) 105.

[9] A. Pardo, J.M.L. Poyato, M.S. Guijarro and J.I.F. Alonso, J. Mol. Spectry. 97 (1983) 248; A. Pardo, J.M.L. Poyato and J.J. Camacho, Spectrochim. Acta 43A (1987) 679.

[10] A. Pardo, J.J. Camacho and J.M.L. Poyato, Chem. Phys. 108 (1986) 15.

[11] G.A. Baker and J.L. Gammel, The Padé approximant in theoretical physics (Academic Press, New York, 1970).

[12] K.D. Jordan, J.L. Kinsey and R. Silbey, J. Chem. Phys. 61 (1974) 911.

[13] V.S. Jorish and N.B. Shcherbak, Chem. Phys. Letters 67 (1979) 160.
[14] G. Herzberg, Molecular spectra and molecular structure, Vol. 1. Spectra of diatomic molecules (Van Nostrand, Princeton, 1950).
[15] J.L. Dunham, Phys. Rev. 41 (1932) 713, 721.
[16] C.R. Vidal and W.C. Stwalley, J. Chem. Phys. 77 (1982) 883.
[17] J.N. Huffaker, J. Chem. Phys. 64 (1976) 3175, 4564.
[18] J.N. Huffaker, J. Mol. Spectry. 71 (1978) 160.
[19] J.J. Camacho, Ph.D. Thesis, Autonoma Madrid University, Spain (1986).
[20] R.C. Weast and M.J. Astle, eds., Handbook of chemistry and physics 63th Ed. (CRC Press, Boca Raton, 1982).
[21] A. Pardo, J.J. Camacho and J.M.L. Poyato, Chem. Phys. Letters 131 (1986) 490.
[22] R.S. Mulliken, Phys. Rev. 50 (1936) 1017, 1028.
[23] A. Pardo, J.J. Camacho and J.M.L. Poyato, Spectrochim. Acta, to be published.